

DC-link voltage balancing in cascaded H-Bridge converters

ARKADIUSZ LEWICKI

Gdansk University of Technology, Faculty of Electrical and Control Engineering
e-mail: alewicki@eia.pg.gda.pl

(Received: 10.03.2014, revised: 08.06.2014)

Abstract: In this paper a DC-link voltage balancing strategy for multilevel Cascaded H-Bridge (CHB) converter is proposed. Presented solution bases on optimal choice of active vector durations in Space-Vector Pulse Width Modulation (SV-PWM). It makes it possible to DC-link voltages control and to properly generate the output voltage vector in the case of DC-link voltage unbalance. Results of simulation and experimental researches on proposed control strategy are presented in the paper.

Key words: cascaded H-Bridge converter, DC-link voltage balancing, space-vector pulse width modulation

1. Introduction

Each phase of multilevel Cascaded H-Bridge Converter (CHB) (Fig. 1) consist of n-H-Bridges (Fig. 2) connected in series. The DC-link circuits of CHB Converter must be galvanically isolated. They can be supplied by rectifiers connected to a multiple winding transformer [1] or to single-phase transformers. It is also possible to supply the DC-link through isolated Dual-Active Bridge (DAB) converters (Fig. 3). These converters are used to electrical energy transfer between DC-links of CHB inverter and CHB rectifier (Fig. 1).

The output voltage of CHB converter is a sum of voltages generated by individual H-bridges. The output voltage can be formed using different modulation strategies, like Sinusoidal Pulse Width Modulation [2], Staircase Modulation [3] or Space-Vector Pulse Width Modulation (SV-PWM) [4, 5].

The SV-PWM strategies for CHB converters usually base on assumption, that the DC-link voltages of H-bridge converters are identical [6, 7]. This assumption makes it easier to identify sectors and sub-sectors in the area, where the output voltage vector is located, and facilitates the selection of active vectors. This area, in seven-level CHB converters (with 3 H-Bridges in any of phases), can be divided into 216 subsectors with the shape of an equilateral triangle. Methods of sub-sector determining are presented in many publications [6, 8-10]. Because any

change in DC-link voltages causes changes in adopted subsectors, it may result in incorrect choice of active voltage vectors and in incorrect generation of output voltage vector in CHB converter.

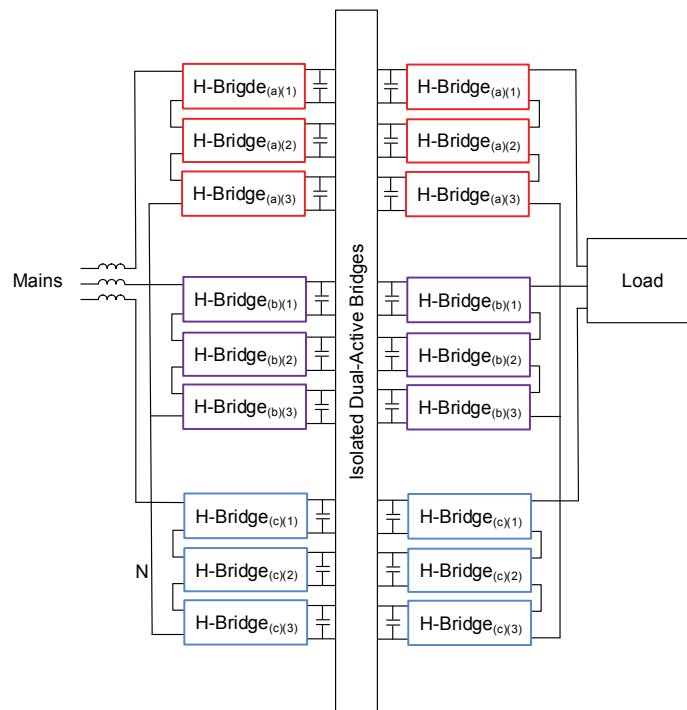


Fig. 1. 7-level H-Bridge Converter

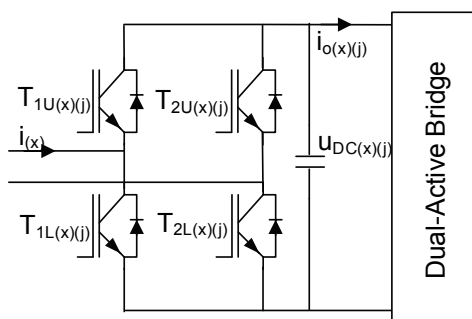


Fig. 2. The j -th H-Bridge ($j = 1 \dots 3$) in the x -phase ($x = a, b$ or c) of a multilevel H-Bridge converter

The CHB converters have to be controlled using modulation strategies which ensure uniform load of each H-Bridge and the same voltages on all DC-link capacitors. In the CHB converters, where DC-links are coupled using DAB converters, uniform load of all H-bridges can be achieved by appropriate choice of converter topology. Isolated DAB converters are used to electrical energy transfer between all phases of a rectifier and all phases of an inverter, like shown in Table 1. In this configuration of 7-level CHB converter the control systems of all 9 DABs work independently. Their task is to maintain equal voltages on both DC-link capacitors (Fig. 3). The disruption in the control system is a voltage change in one of DC-links. It can be caused by current flow through the capacitors during active states in any of H-Bridges (Fig. 3).

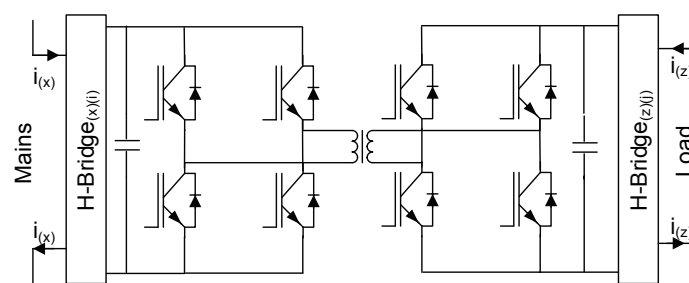


Fig. 3. Dual-Active Bridge in CHB converter topology. x – the phase of CHB rectifier ($x = a, b$ or c), z – the phase of CHB inverter ($z = a, b$, or c)

Table 1. DC-link coupling method of 7-level CHB converter using isolated DC/DC converters (DAB's)

CHB recifier	Coupled with	CHB inverter
H-Bridge _{(a)(1)}	\Leftrightarrow	H-Bridge _{(a)(1)}
H-Bridge _{(b)(1)}	\Leftrightarrow	H-Bridge _{(b)(1)}
H-Bridge _{(c)(1)}	\Leftrightarrow	H-Bridge _{(c)(1)}
H-Bridge _{(a)(2)}	\Leftrightarrow	H-Bridge _{(b)(2)}
H-Bridge _{(b)(2)}	\Leftrightarrow	H-Bridge _{(c)(2)}
H-Bridge _{(c)(2)}	\Leftrightarrow	H-Bridge _{(a)(2)}
H-Bridge _{(a)(3)}	\Leftrightarrow	H-Bridge _{(c)(3)}
H-Bridge _{(b)(3)}	\Leftrightarrow	H-Bridge _{(a)(3)}
H-Bridge _{(c)(3)}	\Leftrightarrow	H-Bridge _{(b)(3)}

If one of passive states is activated in a single H-Bridge, its DC-link voltage does not change. The DC-link voltages of CHB converter can be controlled by swapping the H-Bridges, in which active and passive states are switched-on [4, 11-13]. Such swap can be realised sequentially or in dependence on DC-link voltage unbalance. If the condition (1) is fulfilled:

$$i_{(x)} \cdot u_{o(x)} > 0, \quad (1)$$

where: $i_{(x)}$ is a x -phase current ($x = a, b$ or c) of CHB converter, $i_{(x)} > 0$ denotes that the current is flowing to the converter (Fig. 2), $u_{o(x)}$ is a x -phase reference voltage, obtained using reverse Clarke transformation, the transistors T_{1Ux} and T_{2Lx} are activated when $u_{o(x)} > 0$ (Fig. 2), the CHB converter output voltage is formed using output voltages of H-Bridges with lowest DC-link voltage. The current flow through the DC-links of selected H-Bridges will charge their capacitors. If the condition (1) is not fulfilled, the CHB converter output voltage will be built using H-Bridges with highest DC-link voltages. If the reference voltage is positive, the negative phase current will discharge the capacitors in these H-Bridges, where active states are turned-on.

The DC-link voltages can be also controlled using active redundant states [14, 15]. This method bases on generating of opposite voltages by series connected H-Bridges. Since the sum of these voltages is equal to zero, the converter output voltage does not change. The current flow through these bridge capacitors will change the DC-link voltages. Additional voltages may be also generated by H-Bridges in all CHB converter phases [14]. If voltages in all phases of the converter changes in the same manner, the amplitude and the position of the CHB converter output voltage vector does not change.

In [4] a new SV-PWM strategy for CHB converters was proposed. In this solution the multilevel CHB converter is treated as a series connection of three-level converters. Each of them is formed by three H-Bridges (one H-Bridge in each phase). If the amplitude of output voltage vector of a single three-level converter is too small, the next three H-Bridges are activated. The whole algorithm is repeated until the resulting output voltage vector and the reference voltage vector of CHB converter are not equal. In [4] two different methods for DC-link voltage balancing are utilised. The first one bases on appropriate selection of these H-Bridges, which are utilised to construct the three-level converters. The selection of H-Bridges with active states bases on Equation (1). In other H-Bridges passive states are activated. The second balancing method bases on changes of active state duration in selected H-Bridges. These changes are realised in a manner which ensures proper generating of converter output voltage and reduction of commutation losses. Additionally, simultaneously change of active state durations in three H-Bridges (one H-Bridge in each phase of CHB converter) makes it possible to energy transfer between DC-links of H-Bridges in different phases of CHB converter.

In [4] it was assumed that the three-level inverters are constructed using H-Bridges with lowest DC-link voltages if the condition (1) is fulfilled. If not – the H-bridges with highest DC-link voltages are used as the first. In this paper a development of this control method is proposed. If the condition (1) is fulfilled, the H-Bridges with lowest and highest DC-link voltages are simultaneously considered to use it to construct a single three-level converter. The output voltages of selected 3-level converters form the CHB converter output voltage vector. This solution makes it possible to energy transfer between H-Bridges with lowest and highest DC-link voltages independently on power flow direction. Proposed method requires to prepare of five alternative switching sequences for any sub-sector. The selection method of one of these sequences bases on prediction of DC-link voltage unbalance and prediction of

obtained output voltage vector. The results of simulation and experimental researches are presented in the paper.

2. The duration of active and passive states

The active and passive state durations of any H-Bridge can be calculated from:

$$\begin{aligned} t_{a(x)(i)} &= |\gamma_{(x)(i)}| \cdot T_{\text{pulse}}, \\ t_{p(x)(i)} &= T_{\text{pulse}} - t_{a(x)(i)}, \end{aligned} \quad (2)$$

where: $t_{a(x)(i)}$, $t_{p(x)(i)}$ are the duration of active (a) and passive (p) states of (i) -th H-Bridge in “ x ” phase of CHB converter ($x = a, b$ or c), T_{pulse} is a pulse period.

The duty cycle γ can be calculated from:

$$\gamma_{(x)(i)} = \frac{u_{o(x)(i)}}{u_{DC(x)(i)}} \quad (3)$$

where: $u_{DC(x)(i)}$ is a DC-link voltage of (i) -th H-Bridge in “ x ” phase of CHB converter, $u_{o(x)(i)}$ is an output voltage of this H-Bridge, and:

$$-1 \leq \gamma_{(x)(i)} \leq 1. \quad (4)$$

During passive states ($\gamma_{(x)(i)} = 0$) both upper or both lower H-Bridge transistors are activated (Fig. 2). When one of active states is switched-on, two transistors: $T_{1U(x)(j)}$, $T_{2L(x)(j)}$ (if $(\gamma_{(x)(i)} > 0)$) or $T_{2U(x)(j)}$, $T_{1L(x)(j)}$ (if $(\gamma_{(x)(i)} < 0)$) are activated.

3. Space-Vector Pulse width Modulation

Each three H-Bridges of a multilevel CHB converter (one H-Bridge in one phase) form one 3-level CHB converter. The 7-level CHB converter (Fig. 1) can be considered as a series connection of 3 cascaded three-level converters. The output voltage vector of CHB converter is formed using output voltages of these converters. The components of the output voltage vector can be calculated as:

$$\begin{aligned} u_{o\alpha(ML)} &= \sum_{i=1}^3 u_{o\alpha(3L)(i)}, \\ u_{o\beta(ML)} &= \sum_{i=1}^3 u_{o\beta(3L)(i)}, \end{aligned} \quad (5)$$

where: $u_{o\alpha(ML)}$, $u_{o\beta(ML)}$ are the components of output voltage vector generated in multilevel CHB converter, α, β is the stationary, orthogonal coordinate system, $u_{o\alpha(3L)(i)}$ $u_{o\beta(3L)(i)}$ are components of output voltage vector of three-level converters.

If the (i) -th three-level converter ($1 \leq i \leq 3$) is constructed using: j -th H-Bridge in phase a ($1 \leq j \leq 3$), k -th H-bridge in phase b ($1 \leq k \leq 3$) and m -th H-Bridge in phase c ($1 \leq m \leq 3$), the components of active and passive vectors can be obtained from:

$$\begin{aligned} u_{\alpha(3L)(i)} &= u_{\alpha(a)(j)} + u_{\alpha(b)(k)} + u_{\alpha(c)(m)}, \\ u_{\beta(3L)(i)} &= u_{\beta(a)(j)} + u_{\beta(b)(k)} + u_{\beta(c)(m)}, \end{aligned} \quad (6)$$

where

$$\begin{aligned} u_{\alpha(a)(j)} &= \sqrt{\frac{2}{3}} \cdot u_{DC(a)(j)} \cdot (T_{1U(a)(j)} - T_{2U(a)(j)}), \\ u_{\beta(a)(j)} &= 0, \\ u_{\alpha(b)(k)} &= \sqrt{\frac{2}{3}} \cdot u_{DC(b)(k)} \cdot \cos\left(\frac{2\pi}{3}\right) \cdot (T_{1U(b)(k)} - T_{2U(b)(k)}), \\ u_{\beta(b)(k)} &= \sqrt{\frac{2}{3}} \cdot u_{DC(b)(k)} \cdot \sin\left(\frac{2\pi}{3}\right) \cdot (T_{1U(b)(k)} - T_{2U(b)(k)}), \\ u_{\alpha(c)(m)} &= \sqrt{\frac{2}{3}} \cdot u_{DC(c)(m)} \cdot \cos\left(\frac{4\pi}{3}\right) \cdot (T_{1U(c)(m)} - T_{2U(c)(m)}), \\ u_{\beta(c)(m)} &= \sqrt{\frac{2}{3}} \cdot u_{DC(c)(m)} \cdot \sin\left(\frac{4\pi}{3}\right) \cdot (T_{1U(c)(m)} - T_{2U(c)(m)}), \end{aligned} \quad (7)$$

and: $T_{1U(a)(j)}$, $T_{2U(a)(j)}$, $T_{1U(b)(k)}$, $T_{2U(b)(k)}$, $T_{1U(c)(m)}$, $T_{2U(c)(m)}$ are gate signals of upper transistor (Fig. 2) in a, b and c converter phases (1 – denotes that the upper transistor is switched-on, 0 – denotes that lower transistor is activated), $u_{DC(a)(j)}$, $u_{DC(b)(k)}$, $u_{DC(c)(m)}$ are the DC-link voltages of selected H-Bridges.

The active voltage vectors: $\mathbf{u}_{(a)(j)}$, $\mathbf{u}_{(b)(k)}$, $\mathbf{u}_{(c)(m)}$ are shown on Figure 4.

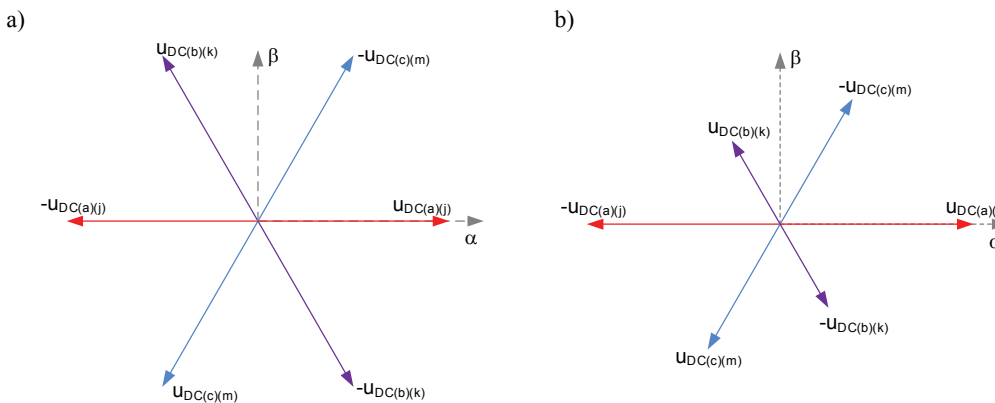


Fig. 4. Amplitude and position of active vectors generated by three H-Bridges (one H-Bridge in each phase of CHB converter) in the case of equal voltages in their DC-links a) and in the case if their DC-link voltages are not equal b)

Because active states can be switched-on simultaneously in each of selected three H-Bridges, the output voltage vector can be located in the area shown in Figure 5. This figure also shows the active voltage vectors obtained in the three-level CHB converter.

The area, where the output voltage vector is localised, can be divided into six sectors spaced $\pi/3$ (Fig. 5). This division facilitates sector determination and selection of assigned active vectors in the case of non-equal DC-link voltages (Fig. 6). The determination of the sector, where the output voltage vector is located, can be based only on this vector angular position.

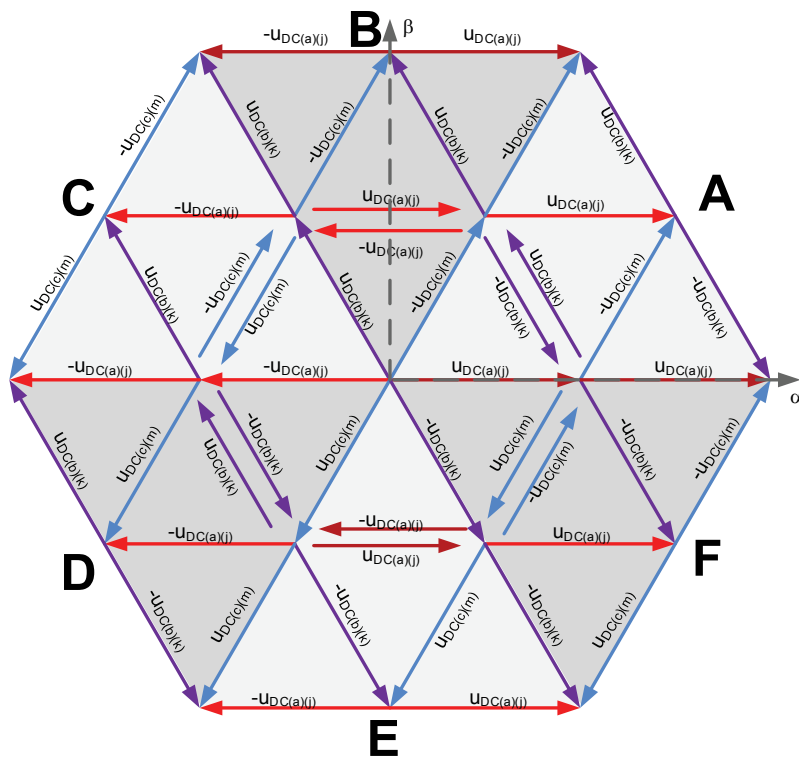


Fig. 5. Active vectors of three-level CHB converter

Modulation I – constructing the output voltage vector using two active vectors

If the output voltage vector of the (i) -th three-level CHB converter will be obtained using two active vectors, active states will be switched-on in two H-Bridges only. In one of selected H-Bridges a passive state will be activated. The selection of these three H-Bridges bases on Equation (1).

The output voltages of selected H-Bridges specify the sector boundaries (Fig. 5, 6a). The duty cycles for two H-Bridges can be calculated using equations:

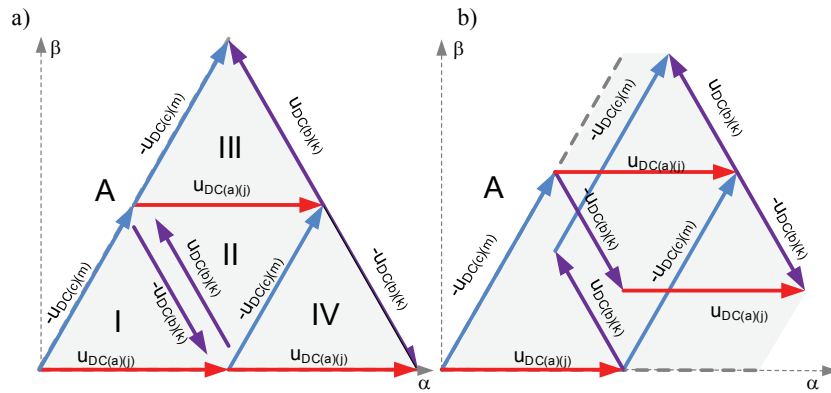


Fig. 6. The shape of sector A in the case of equal voltages in DC-links and in the case if DC-link voltages are not equal

$$\begin{aligned} u_{o\alpha(3L)(i)} &= \gamma_1 \cdot u_{\alpha 1} + \gamma_2 \cdot u_{\alpha 2}, \\ u_{o\beta(3L)(i)} &= \gamma_1 \cdot u_{\beta 1} + \gamma_2 \cdot u_{\beta 2}, \end{aligned} \quad (8)$$

where: $u_{\alpha 1}, u_{\beta 1}, u_{\alpha 2}, u_{\beta 2}$ are the components of active vectors generated in two H-Bridges (6). Equations (8) can be rewritten as:

$$\begin{aligned} \gamma_1 &= \frac{u_{o\alpha(3L)(i)} \cdot u_{\beta 2} - u_{o\beta(3L)(i)} \cdot u_{\alpha 2}}{u_{\beta 2} \cdot u_{\alpha 1} - u_{\alpha 2} \cdot u_{\beta 1}}, \\ \gamma_2 &= \frac{u_{o\beta(3L)(i)} \cdot u_{\beta 2} - u_{o\beta(3L)(i)} \cdot u_{\alpha 2}}{u_{\beta 2} \cdot u_{\alpha 1} - u_{\alpha 2} \cdot u_{\beta 1}}. \end{aligned} \quad (9)$$

If the output voltage vector of CHB converter is located in sector A (Fig. 6), the voltages $u_{DC(a)(j)}$ and $-u_{DC(c)(m)}$ will be used to its construction. Equations (9) can be rewritten as:

$$\begin{aligned} \gamma_{(a)(j)} &= \frac{u_{o\alpha(3L)(i)} \cdot u_{\beta(c)(m)} - u_{o\beta(3L)(i)} \cdot u_{\alpha(c)(m)}}{u_{\beta(c)(m)} \cdot u_{\alpha(a)(j)} - u_{\alpha(c)(m)} \cdot u_{\beta(a)(j)}}, \\ \gamma_{(c)(m)} &= \frac{u_{o\beta(3L)(i)} \cdot u_{\alpha(a)(j)} - u_{o\alpha(3L)(i)} \cdot u_{\beta(a)(j)}}{u_{\beta(c)(m)} \cdot u_{\alpha(a)(j)} - u_{\alpha(c)(m)} \cdot u_{\beta(a)(j)}}. \end{aligned} \quad (10)$$

where a, b, c denotes the phases of CHB converter.

The amplitude of obtained voltage vector depends on its position and on DC-link voltages. If the reference voltage vector is located in subsector III or IV (Fig. 6a), obtained duty cycles are greater than 1. Because the duration of active states cannot exceed the pulse period (2), it may be necessary to reduce determined duty cycles:

$$\text{if } \gamma_{(a)(j)} > 1 \Rightarrow \gamma_{(a)(j)} = 1, \text{ if } \gamma_{(c)(m)} > 1 \Rightarrow \gamma_{(c)(m)} = 1. \quad (11)$$

The components of the output voltage vector, generated in (i) -th three-level CHB converter with the modulation I, can be calculated as:

$$\begin{aligned} u_{o\alpha(3L)(i)(gen)} &= \gamma_{(a)(j)} \cdot u_{\alpha(a)(j)} + \gamma_{(c)(m)} \cdot u_{\alpha(c)(m)}, \\ u_{o\beta(3L)(i)(gen)} &= \gamma_{(a)(j)} \cdot u_{\beta(a)(j)} + \gamma_{(c)(m)} \cdot u_{\beta(c)(m)}. \end{aligned} \quad (12)$$

where $u_{o\alpha(3L)(i)(gen)}$, $u_{o\beta(3L)(i)(gen)}$ are components of the voltage vector, generated in (i) -th three-level CHB converter.

Modulation IIa – constructing the output voltage vector using three active vectors

If the reference voltage vector is located in the sector A (Fig. 5), it can be constructed using following active vectors:

- main active vector: $u_{DC(a)(j)}$,
- complementary active vector: $-u_{DC(c)(m)}$,
- auxiliary active vector: $-u_{DC(b)(k)}$,
- additional active vector: $-u_{DC(a)(z)}$.

Selection of the H-bridges, used to generate the main, complementary and auxiliary active vectors bases on Equation (1). The additional active vector is opposite to the main vector. If the main active vector is generated using H-Bridge with highest DC-link voltage in phase "a" $u_{DC(a)(j)}$, the additional vector will be generated using H-Bridge with lowest DC-link voltage in this phase $u_{DC(a)(z)}$. If the H-Bridge with lowest DC-link voltage $u_{DC(a)(j)}$ will be used to generate the main vector, the H-Bridge with highest DC-link voltage $u_{DC(a)(z)}$ will be selected for additional voltage vector generating.

The duty cycles for H-Bridges, where the main and complementary active vectors are generated, can be calculated using (10). If the duty cycle is less than 1 in the H-Bridge, where the complementary vector is generated (Figs. 7a, 8a), active and passive states will be there activated. The passive states can be eliminated, when the duty cycle γ will be increased to 1 (Figs. 7b, 8b):

$$\text{if } \gamma_{(c)(m)} < 1 \Rightarrow \gamma_{(c)(m)} = 1. \quad (13)$$

The duty cycle increment for the H-Bridge, where the complementary vector is activated, can be calculated as:

$$\Delta\gamma_{(c)(m)} = 1 - \gamma_{(c)(m)}. \quad (14)$$

The change of the duty cycle influences on the amplitude and position of the output voltage vector. The changes of β -component of output voltage vector (Figs. 7b, 8b) can be calculated as:

$$\Delta u_\beta = \Delta\gamma_{(c)(m)} \cdot u_{DC(c)(m)} \sin\left(\frac{\pi}{3}\right), \quad (15)$$

and can be compensated by the auxiliary vector (Figs. 7c, 8c). The duty cycle for the H-Bridge, where the auxiliary voltage vector is generated (Figs. 7c, 8c), can be calculated from:

$$\Delta\gamma_{(b)(k)} = \frac{\Delta u_\beta}{u_{DC(c)(m)} \sin\left(\frac{\pi}{3}\right)}, \quad (16)$$

By substitution (15) to (16) it can be rewritten:

$$\Delta\gamma_{(b)(k)} = \Delta\gamma_{(c)(m)} \frac{u_{DC(c)(m)}}{u_{DC(b)(k)}}. \quad (17)$$

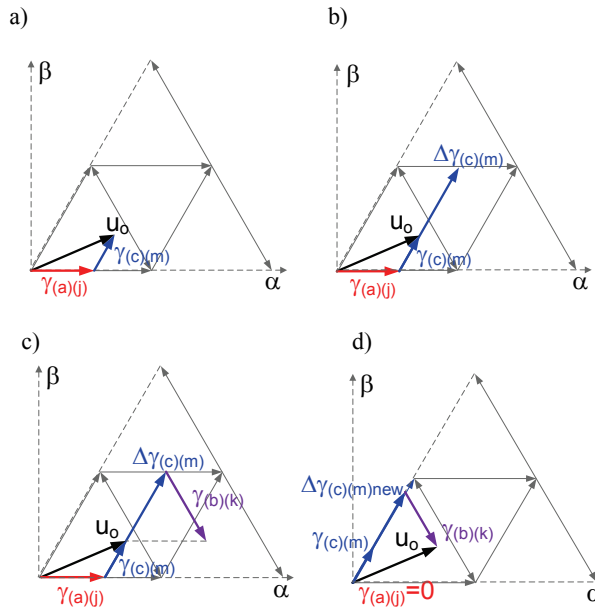


Fig. 7. The steps of duty cycle γ selection in modulation strategy IIa for the case of low amplitude of a reference output voltage vector \mathbf{u}_o

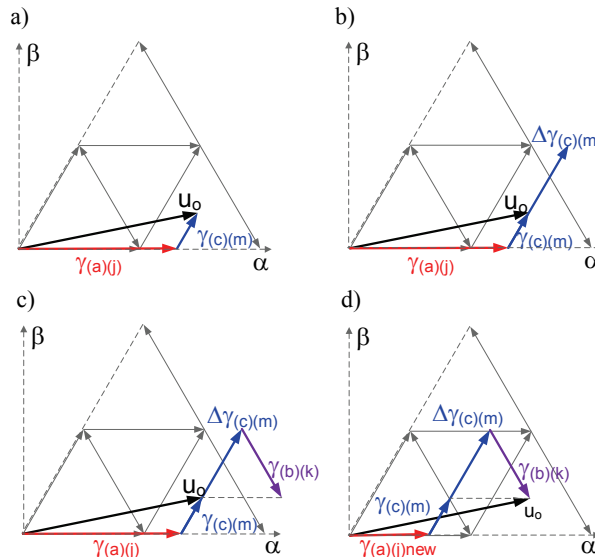


Fig. 8. The steps of duty cycle γ selection in modulation IIa for the case of high amplitude of a reference output voltage vector \mathbf{u}_o

Increasing of the complementary vector duration and activation of the auxiliary vector influences on output voltage vector. The α -component of this vector increases by the value:

$$\Delta u_\alpha = \Delta \gamma_{(c)(m)} \cdot u_{DC(c)(m)} \cdot \cos\left(\frac{\pi}{3}\right) + \Delta \gamma_{(b)(k)} \cdot u_{DC(b)(k)} \cdot \cos\left(\frac{\pi}{3}\right), \quad (18)$$

The new duty cycle for the H-Bridge, where the main voltage vector is generated, can be obtained from (Fig. 8d):

$$\gamma_{(a)(j)\text{new}} = \gamma_{(a)(j)} - \frac{\Delta u_\alpha}{u_{DC(a)(j)}}. \quad (19)$$

If the new value of the duty cycle is negative (Fig. 7d):

$$\gamma_{(a)(j)\text{new}} < 0, \quad (20)$$

it is necessary to reduce the duty cycles for these H-Bridges, where the complementary and auxiliary vectors are generated. Assuming, that:

$$\gamma_{(a)(j)\text{new}} = 0, \quad (21)$$

the new duty cycles for these H-bridges can be calculated from:

$$\begin{aligned} \gamma_{(c)(m)\text{new}} &= \gamma_{(c)(m)} + \Delta \gamma_{(c)(m)\text{new}} = \gamma_{(c)(m)} + \gamma_{(a)(j)} \cdot \frac{u_{DC(a)(j)}}{u_{DC(c)(m)}}, \\ \gamma_{(c)(m)\text{new}} &= \gamma_{(a)(j)} \cdot \frac{u_{DC(a)(j)}}{u_{DC(b)(k)}}. \end{aligned} \quad (22)$$

The position of the main voltage vector is similar to the position of a reference voltage vector. During activation of the main voltage vector the DC-link voltage of (j)-th H-Bridge increases when the condition (1) is fulfilled and otherwise it decreases.

Modulation IIb – constructing the output voltage vector using three active vectors

The modulation strategy IIb is an extension of the modulation strategy IIa for the case, if the condition (20) is fulfilled. In this case the durations of complementary and auxiliary vectors do not change, the duration of main active voltage vector is set to zero and additional voltage vector is activated (Fig. 9).

The direction of the additional voltage vector $-u_{DC(a)(z)}$ is opposite to the converter output voltage vector. Activation of the additional voltage vector will discharge the DC-link capacitor of the z -th H-Bridge when the condition (1) is met, and will charge it when the condition (1) is not fulfilled.

The duty cycle for the H-Bridge, where additional vector is activated, can be calculated as:

$$\gamma_{(a)(z)} = \gamma_{(a)(j)} \cdot \frac{u_{DC(a)(j)}}{u_{DC(b)(k)}}. \quad (23)$$

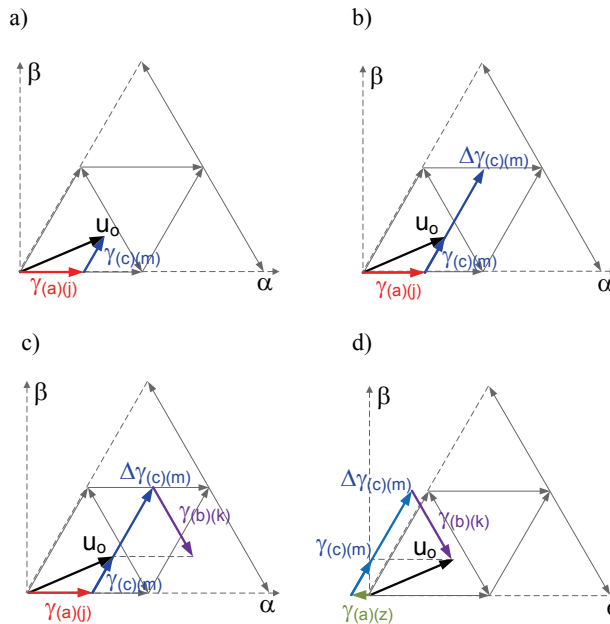


Fig. 9. The steps of duty cycles γ selection in modulation IIb for the case of low amplitude of a reference output voltage vector \mathbf{u}_o

If the duty cycles, determined by modulation strategies IIa or IIb, are greater than 1, it is necessary to limit them:

$$\begin{aligned} \text{if } \gamma_{(a)(j)} > 1 \Rightarrow \gamma_{(a)(j)} = 1, \\ \text{if } \gamma_{(a)(z)} > 1 \Rightarrow \gamma_{(a)(z)} = 1, \\ \text{if } \gamma_{(b)(k)} > 1 \Rightarrow \gamma_{(b)(k)} = 1, \\ \text{if } \gamma_{(c)(m)} > 1 \Rightarrow \gamma_{(c)(m)} = 1. \end{aligned} \quad (24)$$

The components of output voltage vector, generated in i -th three-level CHB converter using modulation strategy IIa or IIb, can be determined from:

$$\begin{aligned} u_{o\alpha(3L)(i)(gen)} &= \gamma_{(a)(j)} \cdot u_{\alpha(a)(j)} + \gamma_{(a)(z)} \cdot u_{\alpha(a)(z)} + \gamma_{(b)(k)} \cdot u_{\alpha(b)(k)} + \gamma_{(c)(m)} \cdot u_{\alpha(c)(m)}, \\ u_{o\beta(3L)(i)(gen)} &= \gamma_{(a)(j)} \cdot u_{\beta(a)(j)} + \gamma_{(a)(z)} \cdot u_{\beta(a)(z)} + \gamma_{(b)(k)} \cdot u_{\beta(b)(k)} + \gamma_{(c)(m)} \cdot u_{\beta(c)(m)}. \end{aligned} \quad (25)$$

Modulation IIIa and IIIb – constructing the output voltage vector using three active vectors

Modulation strategies IIIa and IIIb utilize replaced main and complementary active vector, defined for the modulation strategies IIa and IIb, and modified auxiliary and additional vectors. If the output voltage vector is located in sector A (Fig. 5), the following active vectors will be utilized:

- main active vector: $-u_{DC(c)(m)}$,
- complementary active vector: $u_{DC(a)(j)}$,

- auxiliary active vector: $u_{DC(b)(k)}$,
- additional active vector: $u_{DC(c)(w)}$.

The duty cycles for the selected H-Bridges are determined in the same manner as in modulation strategies IIa and IIb. If the output voltage vector using modulation strategy IIIa is generated, the duty cycles for the j -th H-Bridge in phase a and k -th H-Bridge in phase b are increased, while the duty cycle for the m -th H-Bridge in phase c is reduced. If determined duty cycles are greater than 1, it is necessary to limit them, similarly as in modulation strategy II. The components of the output voltage vector are also determined in the same manner as in modulation strategy II (25).

4. The choice of modulation strategy

Modulation strategies IIa and IIIa make it possible to generate the output voltage vector in whole area shown in Figure 5. The output voltage vector, obtained using modulation strategy I, can be located in subsectors I or II (Fig. 6a), while the modulation strategies IIb and IIIb allow to generate the output voltage vector located in subsector I (Fig. 6a). All modulation strategies make it possible to obtain the duty cycle equal to 1 or 0 in one of H-Bridges of a three-level CHB converter. The passive or active state duration is then equal to a pulse period. If such situation will be maintained for several pulse periods, the converter switching losses will be reduced.

For each of the proposed modulation strategies the DC-link voltages can be predicted using equations:

$$u_{DC(x)(j)}(p+1) = u_{DC(x)(j)}(p) + \frac{1}{C} \cdot \gamma_{(x)(j)} \cdot T_{imp} \cdot i_{(x)}, \quad (26)$$

where indexes (p) and $(p+1)$ denote the actual and next value of DC-link voltages of j -th H-Bridge in phase x ($x = a, b$ or c), C is DC-link capacitance, $i_{(x)}$ is a phase “ x ” current.

The output voltage vector of CHB converter will be generated using this modulation strategy, which ensures minimum value of the function:

$$\begin{aligned} f(u_{DC(a)(j)}, u_{DC(b)(k)}, u_{DC(c)(m)}) = & (u_{DC(a)(j)}(p+1) - u_{DC(AV)})^2 + \\ & + (u_{DC(a)(z)}(p+1) - u_{DC(AV)})^2 + (u_{DC(b)(k)}(p+1) - u_{DC(AV)})^2 + \\ & + (u_{DC(b)(v)}(p+1) - u_{DC(AV)})^2 + (u_{DC(c)(m)}(p+1) - u_{DC(AV)})^2 + \\ & + (u_{DC(c)(w)}(p+1) - u_{DC(AV)})^2, \end{aligned} \quad (27)$$

where:

$$u_{DC(AV)} = \frac{1}{6} \cdot \begin{cases} u_{DC(a)(j)}(p+1) - u_{DC(a)(z)}(p+1) + \\ u_{DC(b)(k)}(p+1) + u_{DC(b)(v)}(p+1) + \\ u_{DC(c)(m)}(p+1) + u_{DC(c)(w)}(p+1) \end{cases}. \quad (28)$$

The criterion (27) is considered for only those strategies, where it is not necessary to limit the duty cycles. If the reference voltage vector is located outside the area shown in Figure 5, it is generated using the modulation strategy which provides minimum value of the following function:

$$f(u_{o\alpha(3L)(gen)}, u_{o\beta(3L)(gen)}) = (u_{o\alpha(ML)} - u_{o\alpha(3L)(gen)})^2 + (u_{o\beta(ML)} - u_{o\beta(3L)(gen)})^2. \quad (29)$$

At the first stage of the control algorithm only one of the n -H-Bridges in each of CHB converter phases is utilised. The next H-bridges will be used to generate the voltage vector with components:

$$\begin{aligned} u'_{o\alpha(ML)} &= u_{o\alpha(ML)} - u_{o\alpha(3L)(gen)}, \\ u'_{o\beta(ML)} &= u_{o\beta(ML)} - u_{o\beta(3L)(gen)}, \end{aligned} \quad (30)$$

where: $u'_{o\alpha(ML)}$, $u'_{o\beta(ML)}$ are the components of a reference voltage vector, generated in next stage of CHB converter.

Proposed algorithm is repeated for next three-level converters as long as the condition (31) is not met:

$$\begin{aligned} u'_{o\alpha(ML)} &= 0, \\ u'_{o\beta(ML)} &= 0. \end{aligned} \quad (31)$$

5. Results of simulation and experimental researches

The simulation researches using Matlab-Simulink were realised. Proposed solution was utilised to control of two seven-level CHB rectifier. The rectifiers were used to couple two mains 3.3 kV. The converter configuration shown in Table 1.

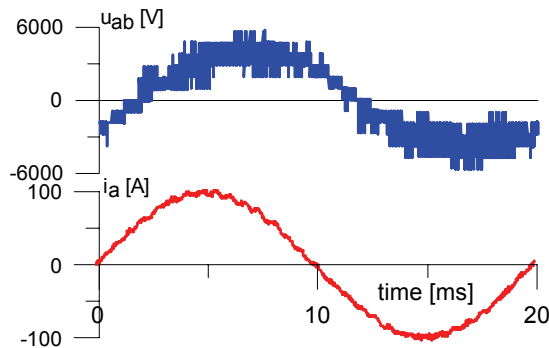


Fig. 10. Phase current and output voltage of 7-level CHB rectifier controlled using proposed SV-PWM strategy

The control systems of both 7-level CHB rectifiers were based on two PI controllers and were not coupled. In both rectifiers the reactive power was set to zero. The phase current and the output voltage of a rectifier is presented in Figure 10.

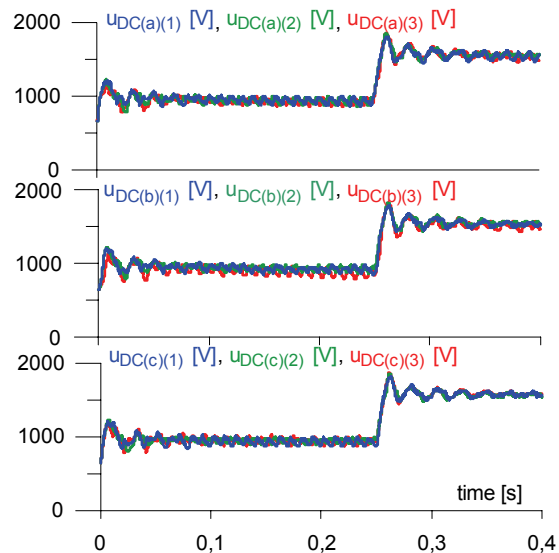


Fig. 11. Step change of DC-link voltages of 7-level CHB rectifier. $u_{DC(x)(i)}$ – the DC-link voltage of (i)-th H-Bridge ($i = 1 \dots 3$) in a “x”-phase ($x = a, b, c$) of CHB converter

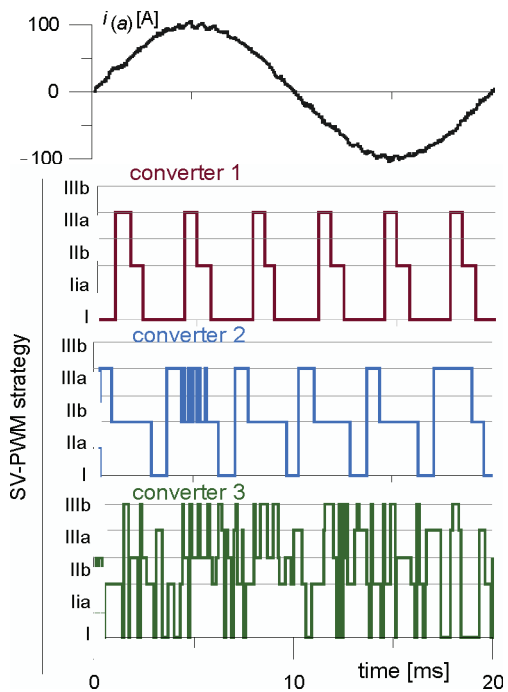


Fig. 12. The SV-PWM modulation strategies used to control of 3-level CHB-convertisers in 7-level CHB rectifier topology

The DC-link voltages of 7-level CHB rectifier during a step change of reference DC-link voltage is shown in Figure 11. The DC-link voltages were controlled using proposed PWM strategy.

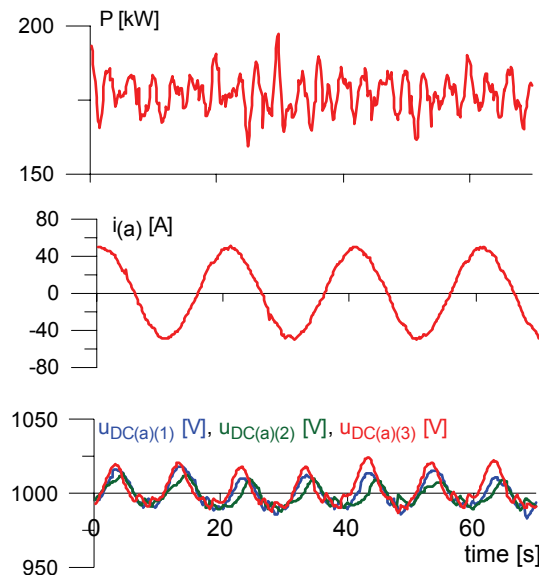


Fig. 13. The phase current $i_{(a)}$, transferred active power P and DC-link voltages $u_{DC(a)(1-3)}$ of all H-Bridges in “a” phase of 7-level CHB converter. Results of experimental researches

Proposed control strategy includes five alternative switching sequences (modulation I, IIa, IIb, IIIa, IIIb) predefined for each of sectors A-E (Fig. 5). The choice of active vectors have to ensure reduction of DC-link voltage unbalance and to ensure appropriate voltage vector to generate. The rectifier phase current and utilised modulation strategies for all three-level converters of 7-level CHB rectifier are shown in Figure 12.

Because of high amplitude of the reference voltage vector the first three-level converter (converter 1/Fig. 12) operates in the overmodulation region. The generated output voltage vector is located on the edge of the area shown in Figure 5. Because the reference voltage vector calculated from (30) is still located outside the area shown in Figure 5, the next converter (converter 2/Fig. 12) also operates in overmodulation mode. In both converters (1 and 2) it is possible to utilize one of three modulation strategies: I, IIa and IIIa. The choice of switching sequence bases on Equation (29), while the choice of H-Bridges used in these 3-level converters bases on Equation (1).

Modulation strategies IIa and IIIa utilizes all three H-bridges of 3-level CHB converter. Modulation I utilizes only two of selected three H-Bridges. All the H-bridges, which were not utilized in two first converters (all H-Bridges with zero duty cycles $\gamma_{(x)(i)} = 0$), can be used to generate the output voltage vector in the last stage of PWM algorithm. The reference voltage vector for the last 3-level converter (converter 3/Fig. 12) is located inside the area shown in Figure 5. All prepared modulation methods can be used there to generate the output voltage vector. The choice of utilized modulation strategy bases on Equation (27).

The experimental researches were carried out on two 7-level rectifiers, used to couple two mains 3.3 kV. The DC-link voltages, phase current and transferred active power are presented in Figure 13.

The results of simulation and experimental researches confirm the correctness of proposed control method. The DC-link voltages in all phases of CHB converter are almost identical.

6. Conclusions

In this paper the SV-PWM strategy for multilevel CHB converter is proposed. Presented solution allows properly generating the inverter output voltage and controlling the DC-link voltages. The DC-link voltages are balanced by appropriate selection of these H-Bridges, where active states are switched on and appropriate selection of active state durations.

Proposed SV-PWM strategy defines five alternative switching sequences for each sectors in the area, where the output voltage is located. The sequence selection bases on prediction of DC-link voltage unbalance and on prediction of obtained voltage vector. This makes it possible to correct generation of an output voltage vector in multilevel CHB converter while the DC-link voltage unbalance is minimized.

References

- [1] Beig A.R., *Constant v/f induction motor drive with synchronised space vector pulse width modulation*. Power Electronics, IET 5(8) (2012).
- [2] Rodríguez J., Bernet S., Wu B. et al., *Multilevel Voltage-Source-Converter Topologies for Industrial Medium-Voltage Driver*. IEEE Transactions On Industrial Electronics 54(6), (2007).
- [3] Zhang Guopeng, Wang Cong, Cheng Hong, Wang Shuo, *Modified Staircase Modulation for Extending Unbalanced Loads Range of Cascaded H-Bridge Rectifier*. Power and Energy Engineering Conference (APPEEC), (2012).
- [4] Lewicki A., *The SV-PWM strategy for multilevel Cascaded H-Bridge converters*. Electrical Review 6 (2013) (in Polish).
- [5] Rabinovici R., Baimel D., Tomaszik J., Zuckerberger A., *Series space vector modulation for multi-level cascaded H-bridge inverters*. Power Electronics IET 3(6): 2010.
- [6] Sanmin Wei, Bin Wu, Fahai Li, Congwei Liu, *A general space vector PWM control algorithm for multilevel inverters*. Eighteenth Annual IEEE Applied Power Electronics Conference and Exposition (APEC), (2003).
- [7] Celanovic N., Boroyevich D., *A fast space-vector modulation algorithm for multilevel three-phase converters*. IEEE Transactions on Industry Applications 37(2): 637-641 (2001).
- [8] Jana K.C., Biswas S.K., Thakura P., *A Simple and Generalized Space Vector PWM Control of Cascaded H-Bridge Multilevel Inverters*. IEEE International Conference on Industrial Technology (ICIT), (2006).
- [9] Kocalmis A., Sunter S., *Simulation of a Space Vector PWM Controller For a Three-Level Voltage-Fed Inverter Motor Drive*. 32nd IEEE Annual Conference on Industrial Electronics, (IECON), (2006).
- [10] Wei S., Wu B., Qianghua Wang, *An improved space vector PWM control algorithm for multilevel inverters*. The 4th International Power Electronics and Motion Control Conference, (IPEMC), (2004).
- [11] Ghazanfari A., Mokhtari H., Firouzi M., *Simple Voltage Balancing Approach for CHB Multilevel Inverter Considering Low Harmonic Content Based on a Hybrid Optimal Modulation Strategy*. IEEE Transactions on Power Delivery 27(4), (2012).
- [12] Guopeng Zhang, Hong Cheng, Cong Wang, Zhichao Xia, *The voltage balance control for new generation of high power cascaded H-bridge rectifier*. 6th IEEE Conference on Industrial Electronics and Applications (ICIEA), (2011).
- [13] Vodden J., Wheeler P., Clare J., *DC link balancing and ripple compensation for a cascaded-H-bridge using space vector modulation*. IEEE Energy Conversion Congress and Exposition, (ECCE), (2009).
- [14] Zygmanowski M., Grzesik B., Michalak J., *Power conditioning system with cascaded H-bridge multilevel converter – DC-link voltage balancing method*. 14th Europe Conference on Power Electronics and Applications, (EPE), (2011).
- [15] Sepahvand H., Jingsheng Liao, Ferdowsi, M., *Investigation on Capacitor Voltage Regulation in Cascaded H-Bridge Multilevel Converters With Fundamental Frequency Switching*. IEEE Transactions on Industrial Electronics 58(11), (2011).